

# An Optuna-Based Metaheuristic Optimization Framework for Biomedical Image Analysis

Thavavel Vaiyapuri

College of Computer Engineering and Sciences, Prince Sattam bin Abdulaziz University, Saudi Arabia  
t.thangam@psau.edu.sa (corresponding author)

Received: 31 March 2025 | Revised: 29 April 2025 | Accepted: 4 May 2025

Licensed under a CC-BY 4.0 license | Copyright (c) by the authors | DOI: <https://doi.org/10.48084/etasr.11234>

## ABSTRACT

The success of Deep Learning (DL) in biomedical imaging heavily relies on optimal hyperparameter selection, which remains a complex and computationally intensive challenge. This paper introduces a metaheuristic-inspired Optuna framework for efficient hyperparameter optimization and validates its effectiveness using U-Net as a case study for brain MRI segmentation, leveraging Bayesian Optimization (BO) with adaptive pruning and Tree-structured Parzen Estimator (TPE). The proposed framework dynamically searches the hyperparameter space to maximize segmentation accuracy while reducing training overhead. The proposed framework adjusts key architectural, training, and regularization parameters, including the number of filters, optimizer, learning rate, and dropout rate, using a well-defined search space. Experimental results on a brain MRI dataset demonstrate that the proposed framework achieved mean scores of 0.941, 0.8763, and 0.983 for Dice Coefficient (DC), Intersection over Union (IoU), and Structural Similarity Index (SSIM), respectively, with 95% confidence intervals. These results confirm Optuna's effectiveness over traditional and metaheuristic baselines and demonstrate its scalability for broader biomedical AI applications.

**Keywords-**hyperparameter optimization; metaheuristic algorithms; Bayesian optimization; Optuna framework; lightweight U-Net; biomedical image analysis; brain MRI segmentation

## I. INTRODUCTION

The integration of Artificial Intelligence (AI) into biomedical imaging has ushered in a new era of medical diagnostics and image analysis [1]. DL models, particularly Convolutional Neural Network (CNN) [2-4] and U-Net [5] architectures, have demonstrated remarkable success in tasks such as tumor segmentation, disease classification, and anomaly detection in medical scans. These next-generation AI systems are transforming healthcare by providing automated and accurate solutions that augment the capabilities of radiologists and clinicians. However, the performance of these models is heavily dependent on the careful selection of hyperparameters, which remains a critical challenge in DL optimization [6, 7]. Identifying the optimal set of hyperparameters is a high-dimensional, non-trivial problem that requires sophisticated tuning to avoid issues such as overfitting, slow convergence, or suboptimal performance [1].

Conventional hyperparameter tuning methods like Grid Search (GS) and random search are computationally inefficient due to their brute-force and non-adaptive nature [8, 9]. By failing to incorporate knowledge from prior evaluations, these methods are slow and impractical for DL models. To address these limitations, metaheuristic algorithms such as Particle Swarm Optimization (PSO) and Genetic Algorithms (GA) have been explored for hyperparameter optimization [10, 11]. Although these methods enable more efficient heuristic-guided searches compared to brute-force approaches, they still demand

significant computational resources and many iterations to converge, rendering them less scalable for large-scale DL applications.

Unlike metaheuristic approaches that rely on heuristic-based exploration, BO-based methods leverage probabilistic models to efficiently identify promising hyperparameter configurations [2]. Among them, Optuna has gained prominence for its ability to combine adaptive sampling with intelligent resource management. Optuna utilizes a TPE to guide the hyperparameter search based on results from previous trials, focusing on computational resources on high-potential configurations for faster convergence. Additionally, it incorporates pruning mechanisms, analogous to exploitation strategies in metaheuristics, which terminate underperforming trials early to optimize resource utilization. Optuna also supports multi-objective optimization, enabling balanced trade-offs between metrics such as accuracy and computational cost [11, 12]. These capabilities position Optuna as a scalable and effective tool for optimizing DL models.

This study proposes a metaheuristic-inspired Optuna framework for efficient hyperparameter optimization in biomedical imaging AI models. As a case study, the framework is applied to U-Net, a state-of-the-art DL model widely used for medical image segmentation. The focus is on brain MRI segmentation, optimizing U-Net's hyperparameters such as dropout rate, number of filters, optimizer type, and learning rate using Optuna's adaptive search strategy. The results show

that the proposed framework enhances segmentation accuracy while reducing training time, highlighting the potential of metaheuristic-inspired optimization in the advancement of biomedical AI.

## II. RELATED WORKS

Recent advances in metaheuristic optimization have significantly enhanced DL performance across medical imaging applications. Heap-based optimization with gray wolf mechanisms has improved the classification accuracy for colorectal cancer, brain tumors, and chest X-rays using deep residual networks [10], while Enhanced Ant Colony Optimization (EACO) with opposition-based learning has demonstrated superior performance in breast cancer classification using ResNet101 [13]. These approaches have shown remarkable adaptability across diverse imaging modalities: the Manta Ray Foraging Optimizer (MRFO) has proven effective for both brain tumor classification [8] and skin cancer detection [14], and Grey Wolf Optimization (GWO) has enhanced diagnostic accuracy in SE-DenseNet ensembles incorporating DL classifiers [6]. Similarly, the Aquila optimizer has advanced breast cancer analysis through combined segmentation and classification using ConvNeXtTiny and DL architectures [7].

However, these methods face persistent limitations in computational efficiency and convergence speed. Recent reviews highlight their limited adaptability across medical imaging tasks and the need for an improved exploration-exploitation balance review [15, 16]. Hybrid approaches such as FTra-UNet [17], HM-EDA [18], and the Archimedes optimization algorithm with hybrid loss functions [19] have enhanced accuracy but retain substantial computational overhead. Even advanced variants, such as the polynomial Chebyshev symmetric chaotic golden jackal optimizer [20], struggle with scalability in clinical implementations.

In contrast, Bayesian-Optimization (BO) frameworks have emerged as more computationally efficient alternatives for hyperparameter optimization. Recent studies have demonstrated the effectiveness of BO techniques, particularly Optuna, in applications such as necrotizing fasciitis detection [2], breast cancer classification [21], and Alzheimer's disease prediction from MRI data [12]. Beyond Optuna, other frameworks like HyperOpt and SMAC3 have also been widely adopted in machine learning. Table I provides a comparative overview that highlights key differences in surrogate modeling, pruning strategies, and scalability. Compared to HyperOpt and SMAC3, Optuna offers integrated dynamic pruning and adaptive sampling, making it more suitable for computationally intensive biomedical image segmentation tasks [2, 12]. Based on these advantages and its proven success in biomedical applications, Optuna was selected as the optimization framework for this study.

Building on these advances, this study introduces an Optuna-based framework for biomedical AI hyperparameter optimization. The framework leverages Optuna's core capabilities, including adaptive search space exploration, intelligent trial pruning mechanisms, and efficient Bayesian sampling strategies to achieve optimal hyperparameter

configurations. Through a comprehensive evaluation on the U-Net architecture for brain MRI segmentation, this study aims to demonstrate how Optuna can serve as a computationally feasible alternative to traditional metaheuristic-based hyperparameter tuning while maintaining high segmentation accuracy.

TABLE I. COMPARISON OF BO-BASED OPTIMIZATION FRAMEWORKS

Aspects	Optuna	HyperOpt	SMAC3
Surrogate model	TPE	TPE	Random forest
Pruning	dynamic	No	No
Sampling	Adaptive	Sequential	Model-based
Scalability	High	Moderate	Low

## III. METHODOLOGY

The problem is formulated as an objective-driven search to maximize segmentation performance. Next, the proposed framework uses BO with TPE for adaptive hyperparameter sampling and early pruning.

### A. Problem Formulation

The objective is to find the optimal hyperparameters ( $\lambda^*$ ) that maximize a model's segmentation performance (e.g., Dice Coefficient - DC), which can be mathematically represented as,

$$\lambda^* = \operatorname{argmax}_{\lambda \in \Lambda} f(\lambda) \quad (1)$$

where  $\Lambda$  represents the predefined hyperparameter search space and  $f(\lambda)$  is the validation performance metric. Since  $f(\lambda)$  is noisy, non-differentiable, and costly to evaluate, traditional methods, such as GS, are inefficient. Instead, metaheuristic approaches (e.g., PSO) use adaptive sampling to dynamically refine the search, improving optimization efficiency.

### B. Proposed Framework

The proposed framework integrates Optuna as a metaheuristic-driven optimizer to automate the search for optimal hyperparameters in biomedical image segmentation models, as shown in Figure 1. Instead of relying on exhaustive evaluations, Optuna incorporates BO with TPE to intelligently navigate the hyperparameter space through four key phases:

1. Define the Hyperparameter Search Space: The optimization process begins with defining an appropriate search space that encompasses key hyperparameters influencing model performance, including architectural choices such as the number of layers and filters, training parameters like learning rate and batch size, and regularization techniques including dropout rate and weight decay. Continuous parameters are sampled from uniform or log-uniform distributions, while categorical parameters are selected from predefined discrete sets, ensuring flexibility across different models and tasks.
2. Metaheuristic-Based Sampling Strategy with TPE: Unlike brute-force methods such as GS or random search, TPE dynamically models hyperparameter values by maintaining two probabilistic models:  $P(x|y < y^*)$  for high-performing configurations, and  $P(x|y \geq y^*)$  for low-

performing ones. TPE refines these distributions and selects the next hyperparameter configuration  $x^*$  by maximizing the likelihood ratio [12, 21]:

$$x^* = \operatorname{argmax} \frac{P(x|y < y^*)}{P(x|y \geq y^*)} \quad (2)$$

This Bayesian approach balances the exploration of uncertain regions with the exploitation of known high-performing values, optimizing efficiency by avoiding unpromising trials [2]. The adaptive process makes TPE a powerful metaheuristic optimizer.

3. Trial Execution and Dynamic Pruning: Each sampled hyperparameter configuration  $\lambda_i$  undergoes training for a set number of epochs. During training, Optuna applies dynamic pruning to terminate trials that are unlikely to outperform the current best. At predefined checkpoints, the validation DC,  $f(x_i)$  is evaluated, and a trial is pruned if it satisfies [12]:

$$f(x_i) > f(x_{best}) + \delta \quad (3)$$

where  $f(x_{best})$  is the best score observed so far, and  $\delta$  is a small margin to prevent premature termination due to minor fluctuations. This adaptive pruning strategy significantly reduces computational overhead while guiding the search toward more promising hyperparameter regions.

4. Final Hyperparameter Selection: Once all trials are completed, the best-performing hyperparameter configuration is selected as [2]:

$$\lambda^* = \operatorname{argmax}_{\lambda_i} f(\lambda_i) \quad (4)$$

where  $\lambda^*$  corresponds to the hyperparameter configuration that achieves the highest validation performance. The final model is then retrained using  $\lambda^*$  to maximize segmentation accuracy while ensuring computational efficiency.

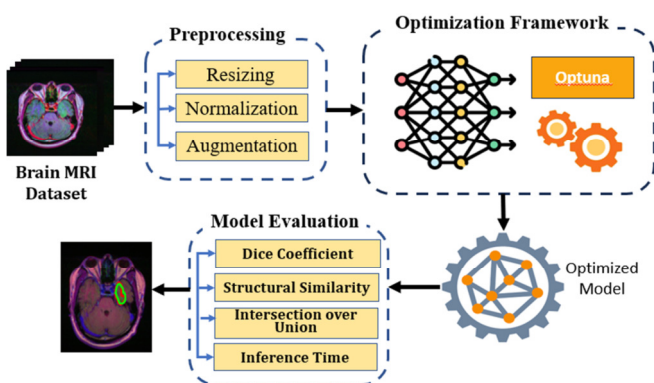


Fig. 1. Proposed metaheuristic-inspired optuna framework for biomedical AI.

Although TPE is grounded in BO, its operation inherently mirrors metaheuristic principles. The balance between exploration and exploitation in TPE parallels strategies found in algorithms such as PSO and Simulated Annealing (SA),

where search agents dynamically balance global exploration and local refinement. Furthermore, the dynamic pruning mechanism in Optuna serves a similar role to exploitation phases in metaheuristics, aggressively focusing resources on high-potential trials, analogous to selection pressure in evolutionary algorithms. Thus, the proposed framework leverages both probabilistic modeling and metaheuristic-inspired adaptive search strategies to optimize hyperparameters efficiently.

## IV. EXPERIMENTAL SETUP

### A. Dataset Description

This study uses a publicly available brain MRI dataset derived from The Cancer Genome Atlas Low-Grade Glioma (TCGA-LGG) [22], designed to support cancer research and explore genotype-phenotype relationships in medical imaging. The dataset was processed and released for use in medical image segmentation tasks [22, 23]. The dataset comprises 3,929 axial slices (256x256 resolution) from 110 LGG patients, including 1,373 tumor and 2,556 non-tumor images, accompanied by manual tumor masks. It is split into 70% for training and 30% for testing, providing a solid benchmark for evaluating tumor segmentation performance. Figure 2 illustrates sample MRI slices.

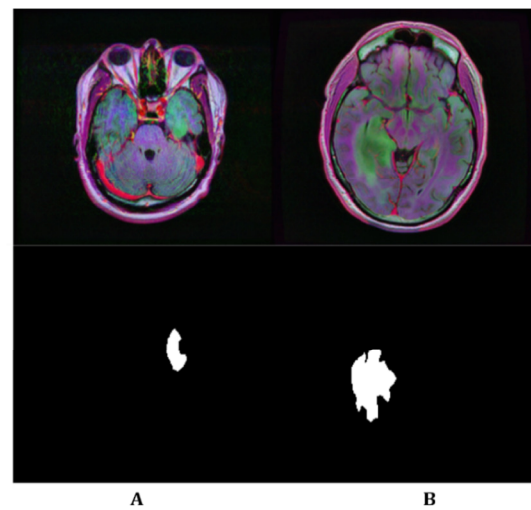


Fig. 2. Sample brain MRI slices (top) and corresponding GT masks (bottom).

### B. Data Preprocessing

All brain MRI slices and corresponding masks were resized to 224x224 pixels and normalized to a [0, 1] range. To enhance generalization, the training data underwent real-time augmentation, including random rotations ( $\pm 0.4$  radians), shifts (5%), shearing (0.02), zooming ( $\pm 4\%$ ), and vertical flips applied consistently to both images and masks using a fixed seed [23]. The test set was left unaltered to ensure unbiased evaluation.

### C. U-Net as a Case Study for Brain MRI Segmentation

DL has revolutionized biomedical image segmentation by enabling automated and precise delineation of anatomical and pathological regions. Among various DL architectures, U-Net, with its encoder-decoder structure and Skip Connections (SC), effectively preserves spatial detail while capturing essential contextual information [5, 24]. This study adopted U-Net as a benchmark architecture to evaluate the effectiveness of Optuna-driven hyperparameter optimization in brain MRI segmentation tasks.

The U-Net architecture, shown in Figure 3, consists of four encoder and decoder blocks, a bottleneck, and SC that retain fine-grained features. Each encoder block includes convolutional layers with ReLU activation, optional batch normalization, max pooling, and dropout. The decoder uses transposed convolutions for upsampling. A final  $1 \times 1$  convolution with sigmoid activation generates the binary segmentation mask. The model was trained using Binary Cross-Entropy (BCE) loss, and performance was evaluated using DC, which quantifies the overlap between predicted ( $P_i$ ) and ground truth ( $G_i$ ) masks [24, 25].

$$DC = \frac{2 \sum_i P_i G_i}{\sum_i P_i + \sum_i G_i} \quad (5)$$

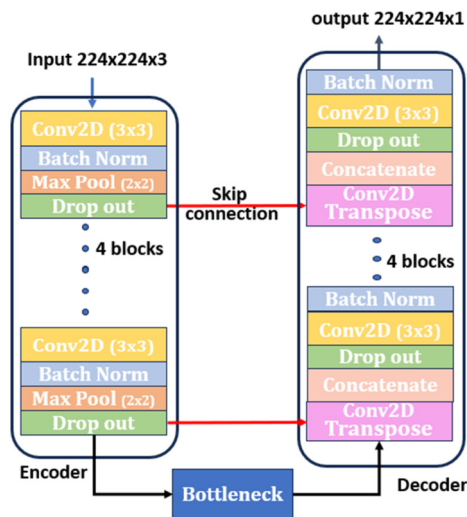


Fig. 3. Schematic of the U-Net architecture

To evaluate the effectiveness of hyperparameter optimization, this study tunes key components of the U-Net model across three categories: architectural (number of filters, which scale through the network), training (optimizer and learning rate), and regularization (dropout rate). These parameters are treated as tunable variables and optimized using the proposed metaheuristic-inspired Optuna framework, as detailed in the methodology section. This approach enables the model to dynamically adjust its learning capacity and regularization strategy, leading to improved segmentation performance, particularly in the complex domain of brain MRI analysis.

### D. Hyperparameter Optimization Details

Building on the U-Net model described above, Optuna was utilized to optimize key hyperparameters that encompass architectural, training, and regularization aspects [26]. The search space included the following:

1. Number of Filters ( $n\_filters$ ): Categorical values, determining the representational capacity at each U-Net level.
2. Dropout Rate ( $dropout$ ): Uniformly sampled from [0.1, 0.5] to control overfitting.
3. The optimizer was chosen between Adam and SGD to explore different update dynamics.
4. Learning Rate: Log-uniformly sampled from [1e-4, 1e-2], allowing fine-grained tuning of convergence behavior.

A total of 15 trials were conducted, each with a unique hyperparameter combination. Optuna's pruning mechanism was applied to discard underperforming trials early, enhancing efficiency. The best-performing configuration was selected for retraining and final evaluation, illustrating the effectiveness of the proposed optimization framework in improving segmentation performance.

## V. RESULTS AND DISCUSSION

### A. Hyperparameter Optimization Evaluation

This section evaluates the effectiveness of Optuna in optimizing U-Net hyperparameters by analyzing trial convergence behavior and the role of dynamic pruning. It also examines how individual parameters affect segmentation performance.

#### 1) Optimization Behavior and Trial Performance

To assess the optimization dynamics of the proposed Optuna-based framework, the optimization history across 15 trials is visualized in Figure 4, where the y-axis represents the objective value (DC) and the x-axis tracks the number of trials. Each blue dot corresponds to the validation performance of a trial, and the red curve traces the best value observed up to each point. The best-performing trial is highlighted with a red circle.

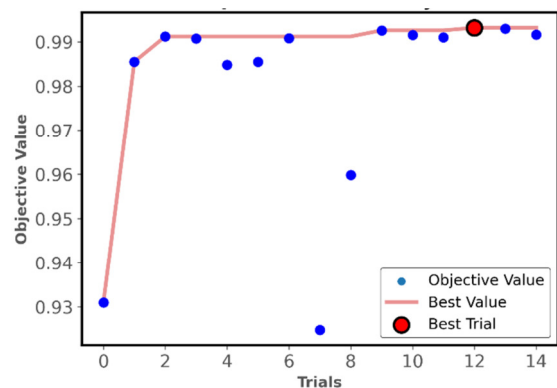


Fig. 4. Optimization history of U-Net using the proposed Optuna framework.

The results show that the objective value improved rapidly within the first few trials, with a plateau observed from trial 3, suggesting a rapid convergence of the search process. While some trials underperformed (e.g., trial 7), the pruning mechanism effectively avoided wasting resources on poor configurations. The best configuration was achieved at trial 13 with a DC score exceeding 0.99, demonstrating the effectiveness and efficiency of the metaheuristic-inspired optimization approach in discovering high-performing hyperparameter combinations.

2) Hyperparameter Impact Analysis

To gain deeper insight into the impact of each hyperparameter on segmentation performance, slice plots were generated for the four parameters tuned during optimization: dropout rate, learning rate, number of filters, and optimizer type. In Figure 5, each subplot illustrates the relationship between a hyperparameter and the corresponding DC score, with the best-performing configuration marked in red. The

results show that a dropout rate of around 0.44 yielded the best performance, suggesting that moderate regularization improves generalization. A low learning rate (0.0003) promoted stable convergence on limited data. Models using 32 filters captured more detailed features than those with 16, and Adam consistently outperformed SGD due to its adaptive learning dynamics. These findings demonstrate Optuna's ability to identify synergistic hyperparameter combinations that improve segmentation accuracy while providing transparency on parameter sensitivity.

B. Optimized U-Net Model Performance Evaluation

1) Qualitative Performance Analysis

To evaluate segmentation performance qualitatively, the results from two brain MRI slices (A and B, shown in Figure 2) were analyzed across four model configurations: baseline (unoptimized), GS-optimized, PSO-optimized, and the proposed Optuna-optimized model (Figure 6).

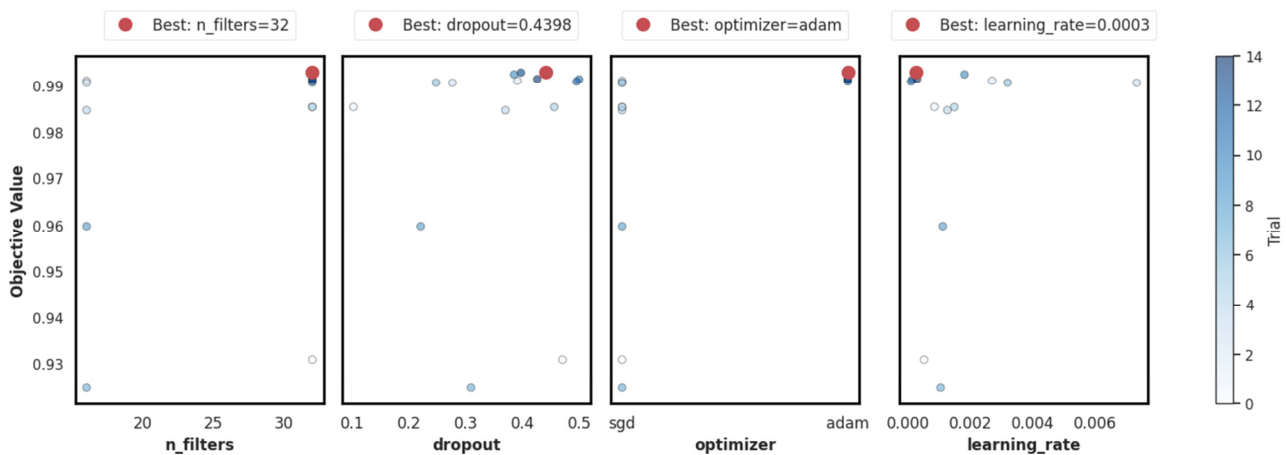


Fig. 5. Slice plots showing the impact of hyperparameter optimization on DC score across Optuna trials.

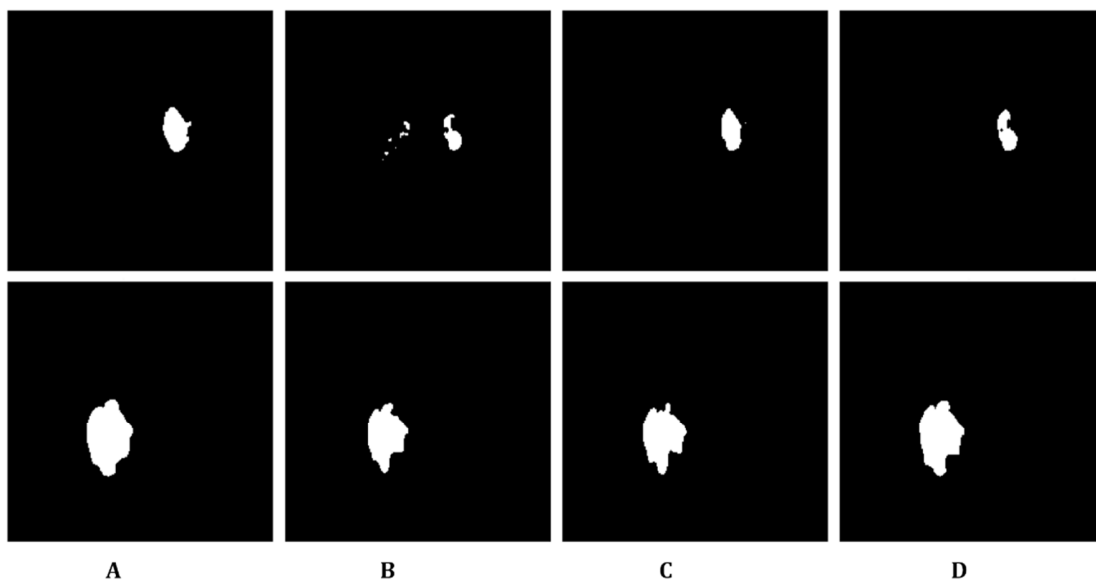


Fig. 6. Segmentation results on two brain MRI samples comparing four approaches: (A) Unoptimized, (B) GS, (C) Metaheuristic-PSO, and (D) Proposed Optuna model.

The baseline U-Net demonstrated broad tumor region detection but exhibited limited boundary precision. The GS-optimized model produced fragmented and noisy segmentation masks, particularly evident in sample A, suggesting suboptimal hyperparameter tuning. The PSO-optimized model showed structural improvements over GS but still failed to capture fine-grained details and maintain edge continuity. In contrast, the Optuna-optimized model consistently produced cleaner and

more accurate masks that closely match ground-truth annotations. In sample A, it maintained compact tumor boundaries with minimal noise, while in sample B, it demonstrated smoother and more complete segmentation of the tumor region. These visual comparisons validate the effectiveness of the proposed hyperparameter tuning approach in enhancing segmentation quality, especially in capturing fine structures and reducing false positives.

TABLE II. PERFORMANCE METRICS OF THE U-NET MODEL COMPARING FOUR DIFFERENT OPTIMIZATION APPROACHES

Model variants	Sample Brain MRI (A)				Sample Brain MRI (B)			
	DC	IoU	SSIM	IT	DC	IoU	SSIM	IT
Unoptimized	0.6873	0.5236	0.9716	0.1407	0.8845	0.7929	0.9647	0.0992
Grid Search (GS)	0.8000	0.6667	0.9830	0.1086	0.9236	0.8581	0.9728	0.1009
Meta-heuristic PSO	0.8089	0.6791	0.9830	0.1468	0.9183	0.8489	0.9724	0.0990
Proposed model	0.8851	0.7938	0.9884	0.1080	0.9359	0.8795	0.9736	0.0680

## 2) Quantitative Performance Analysis

To objectively assess segmentation performance, Table II summarizes four evaluation metrics, DC, IoU, SSIM, and Inference Time (IT), for the two brain MRI samples across four strategies: unoptimized, GS-optimized, PSO-optimized, and the proposed Optuna-based optimization method. The Optuna-optimized model outperformed all baselines in both samples. In sample A, it achieved the highest DC (0.8851) and IoU (0.7938) scores, indicating superior segmentation results and overlap with ground-truth. SSIM was also the highest, reflecting better structural fidelity, while the inference time was kept low (0.1080), showing computational efficiency. Similarly, in sample B, the proposed model recorded the best scores across all metrics, including a DC of 0.9359 and the lowest inference time (0.0680), confirming its ability to generalize across varying inputs. These results validate that Optuna-based tuning not only enhances segmentation precision but also improves structural consistency and runtime performance, making it well-suited for real-time biomedical imaging applications.

## 3) Statistical Performance Analysis

To ensure the reliability of the performance comparisons between different model variants, a statistical analysis was conducted based on 95% confidence intervals for DC, IoU, and SSIM metrics. The mean values and confidence intervals for unoptimized, GS, PSO, and the proposed Optuna-based model are given in Table III and visualized in Figure 7.

TABLE III. PERFORMANCE METRICS WITH 95% CONFIDENCE INTERVAL FOR U-NET COMPARING FOUR DIFFERENT OPTIMIZATION APPROACHES

Optimization approach	DC	IoU	SSIM
Unoptimized	0.7826 [0.6458–0.8932]	0.7264 [0.5706–0.8127]	0.9611 [0.9407–0.9783]
GS	0.8819 [0.6875–0.9244]	0.8038 [0.5942–0.8740]	0.9678 [0.9636–0.9894]
PSO	0.9208 [0.7916–0.9577]	0.8291 [0.6256–0.8913]	0.9765 [0.9683–0.9848]
Proposed	h	0.8763 [0.7627–0.9294]	0.9839 [0.9771–0.9906]

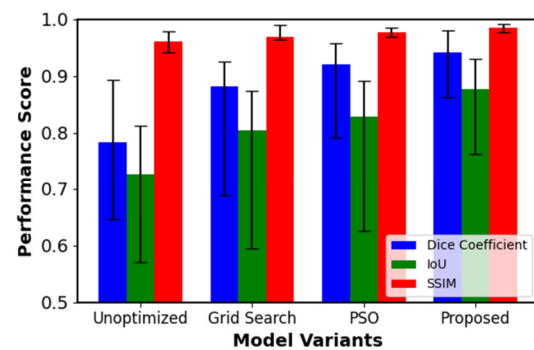


Fig. 7. Optimization history of U-Net using the proposed Optuna framework.

The results show that the proposed model consistently achieved higher mean scores of 0.941, 0.8763, and 0.983 for DC, IoU, and SSIM, respectively, with narrower confidence intervals compared to baseline methods. This demonstrates not only superior segmentation accuracy but also reduced variability across test samples, reinforcing the statistical robustness of the improvements achieved through the proposed hyperparameter optimization framework.

## C. Performance Comparison with Related Works

The segmentation performance of the proposed Optuna-optimized U-Net model was compared with several recent approaches, as summarized in Table IV, using DC and IoU as evaluation metrics.

TABLE IV. PERFORMANCE COMPARISON WITH RELATED WORKS

Ref.	DL Model Used	DC	IoU
[3]	U-Net + FPN	0.92	0.86
[24]	U-Net + ResNet50	0.891	0.883
[27]	U-Net + Vgg16	0.9181	0.8264
[5]	U-Net + DA	0.9158	-
[28]	U-Net + EfficientNetB7	0.9387	0.9174
Proposed	Optuna Optimized U-Net	0.9415	0.8963

The U-Net improved with Feature Pyramid Networks (FPN) [3] achieved a DC of 0.92 and IoU of 0.86 but exhibited limited adaptability to complex tumor structures. U-Net with

ResNet-50 [24] achieved a DC of 0.891 and IoU of 0.883, reflecting moderate multi-scale feature handling. The VGG16-based U-Net [27] reported a higher DC (0.9181) but a lower IoU (0.8264), indicating challenges in fine boundary segmentation. Znet [5] incorporated U-Net with SC and data augmentation to achieve a DC of 0.9158, though with a slightly lower IoU. EffUNet++-TL [28], combining EfficientNetB7 with U-Net++, demonstrated strong results (DC 0.9387, IoU 0.9174) through enhanced multi-scale feature fusion. In comparison, the proposed model achieved the highest DC (0.9415) while maintaining a competitive IoU (0.8963), confirming its superior accuracy in brain tumor segmentation.

## VI. CONCLUSION

This study demonstrated that the proposed Optuna-based framework provides a computationally efficient and effective solution for hyperparameter optimization in biomedical AI applications. Using U-Net as a case study for brain MRI segmentation, the framework identified optimal combinations of architectural, training, and regularization parameters. The optimized model achieved a DC of 0.94, significantly outperforming traditional GS and PSO-based methods in both qualitative and quantitative evaluations. These results underscore the framework's ability to enhance segmentation accuracy, generalization, and computational efficiency. Overall, the findings validate the practical value of metaheuristic-inspired BO for advancing next-generation AI systems in healthcare.

Although the proposed framework demonstrated strong optimization performance, it was evaluated primarily on 2D medical images. Extending it to 3D volumetric data and scaling to larger models, such as Vision Transformers (ViT), would introduce additional computational and memory challenges. Future work will focus on adapting the framework to address these challenges and incorporating multi-objective strategies to balance accuracy, model size, and inference latency for deployment in resource-constrained environments. Furthermore, experimental comparisons with other optimization frameworks, such as HyperOpt and SMAC3, will be explored to further validate and benchmark performance. Ethical considerations must also be acknowledged, as public datasets such as TCGA may exhibit demographic biases and institutional variability, potentially limiting model generalizability. Addressing these concerns by integrating more diverse datasets and applying fairness-aware optimization techniques will also be a priority for future research.

## ACKNOWLEDGMENT

The author extends her appreciation to Prince Sattam bin Abdulaziz University for funding this research work through project number PSAU/2024/01/29695.

## REFERENCES

[1] E. H. Houssein, E. Saber, A. A. Ali, and Y. M. Wazery, "Integrating metaheuristics and artificial intelligence for healthcare: basics, challenging and future directions," *Artificial Intelligence Review*, vol. 57, no. 8, Jul. 2024, Art. no. 205, <https://doi.org/10.1007/s10462-024-10822-2>.

[2] M. J. Tsai, C. H. Lin, J. P. Lai, and P. F. Pai, "Using Deep Learning, Optuna, and Digital Images to Identify Necrotizing Fasciitis,"

*Electronics*, vol. 13, no. 22, Jan. 2024, Art. no. 4421, <https://doi.org/10.3390/electronics13224421>.

[3] H. Sun *et al.*, "Brain tumor image segmentation based on improved FPN," *BMC Medical Imaging*, vol. 23, no. 1, Oct. 2023, Art. no. 172, <https://doi.org/10.1186/s12880-023-01131-1>.

[4] T. H. Tran, P. A. Nguyen, L. A. Ngoc, D. T. Tran, and M. T. Pham, "Optimal CNN Model for Obstructive Sleep Apnea Detection using Particle Swarm Optimization," *Engineering, Technology & Applied Science Research*, vol. 15, no. 1, pp. 19553–19560, Feb. 2025, <https://doi.org/10.48084/etasr.9154>.

[5] M. A. Ottom, H. A. Rahman, and I. D. Dinov, "Znet: Deep Learning Approach for 2D MRI Brain Tumor Segmentation," *IEEE Journal of Translational Engineering in Health and Medicine*, vol. 10, pp. 1–8, 2022, <https://doi.org/10.1109/JTEHM.2022.3176737>.

[6] S. Adamu *et al.*, "Unleashing the power of Manta Rays Foraging Optimizer: A novel approach for hyper-parameter optimization in skin cancer classification," *Biomedical Signal Processing and Control*, vol. 99, Jan. 2025, Art. no. 106855, <https://doi.org/10.1016/j.bspc.2024.106855>.

[7] M. Sreevani and R. Latha, "A Deep Learning with Metaheuristic Optimization-Driven Breast Cancer Segmentation and Classification Model using Mammogram Imaging," *Engineering, Technology & Applied Science Research*, vol. 15, no. 1, pp. 20342–20347, Feb. 2025, <https://doi.org/10.48084/etasr.9406>.

[8] M. Aljohani *et al.*, "An automated metaheuristic-optimized approach for diagnosing and classifying brain tumors based on a convolutional neural network," *Results in Engineering*, vol. 23, Sep. 2024, Art. no. 102459, <https://doi.org/10.1016/j.rineng.2024.102459>.

[9] T. Vaiyapuri, "Utilizing Explainable AI and Biosensors for Clinical Diagnosis of Infectious Vector-Borne Diseases," *Engineering, Technology & Applied Science Research*, vol. 14, no. 6, pp. 18640–18648, Dec. 2024, <https://doi.org/10.48084/etasr.9026>.

[10] L. Zhang, Z. Qiao, and L. Li, "An Evolutionary Deep Learning Method Based on Improved Heap-Based Optimization for Medical Image Classification and Diagnosis," *IEEE Access*, vol. 12, pp. 102745–102773, 2024, <https://doi.org/10.1109/ACCESS.2024.3433483>.

[11] T. Vaiyapuri, H. Alaskar, Z. Sbai, and S. Devi, "GA-based multi-objective optimization technique for medical image denoising in wavelet domain," *Journal of Intelligent & Fuzzy Systems*, vol. 41, no. 1, pp. 1575–1588, Aug. 2021, <https://doi.org/10.3233/JIFS-210429>.

[12] P. Deepan, G. Prabhakar Reddy, M. Arsha Reddy, R. Vidya, and S. Dhiravidaselvi, "Maximizing Accuracy in Alzheimer's Disease Prediction: A Optuna Hyper Parameter Optimization Strategy Using MRI Images," in *Revolutionizing Healthcare 5.0: The Power of Generative AI: Advancements in Patient Care Through Generative AI Algorithms*, P. Bhattacharya, H. Liu, P. K. Dutta, J. J. P. C. Rodrigues, and G. Sethi, Eds. Springer Nature Switzerland, 2024, pp. 77–91.

[13] S. Thirumalaisamy *et al.*, "Breast Cancer Classification Using Synthesized Deep Learning Model with Metaheuristic Optimization Algorithm," *Diagnostics*, vol. 13, no. 18, Jan. 2023, Art. no. 2925, <https://doi.org/10.3390/diagnostics13182925>.

[14] J. D. Dorathi Jayaseeli *et al.*, "An intelligent framework for skin cancer detection and classification using fusion of Squeeze-Excitation-DenseNet with Metaheuristic-driven ensemble deep learning models," *Scientific Reports*, vol. 15, no. 1, Mar. 2025, Art. no. 7425, <https://doi.org/10.1038/s41598-025-92293-1>.

[15] M. K. Bohmrah and H. Kaur, "Advanced Hybridization and Optimization of DNNs for Medical Imaging: A Survey on Disease Detection Techniques," *Artificial Intelligence Review*, vol. 58, no. 4, Feb. 2025, Art. no. 122, <https://doi.org/10.1007/s10462-024-11049-x>.

[16] Q. S. Hamad, H. Samma, and S. A. Suandi, "Optimization of Convolutional Neural Network Hyperparameter for Medical Image Diagnosis using Metaheuristic Algorithms: A short Recent Review (2019-2022)," arXiv, Dec. 23, 2024, <https://doi.org/10.48550/arXiv.2412.17956>.

[17] J. Nithisha *et al.*, "Fuzzy Hybrid Meta-optimized Learning-based Medical Image Segmentation System for Enhanced Diagnosis," *International Journal of Information Technology and Computer Science*,

- vol. 17, no. 1, pp. 47–66, Feb. 2025, <https://doi.org/10.5815/ijitcs.2025.01.04>.
- [18] N. Bansal and A. Vidyarthi, "Hierarchical Meta-Heuristic Encoder-Decoder Architecture With Next-Generation Imaging for Consumer-Centric Segmentation of Diabetic Foot Ulcers," *IEEE Transactions on Consumer Electronics*, pp. 1–1, 2025, <https://doi.org/10.1109/TCE.2025.3532639>.
- [19] H. M. Balaha *et al.*, "AOA-guided hyperparameter refinement for precise medical image segmentation," *Alexandria Engineering Journal*, vol. 120, pp. 547–560, May 2025, <https://doi.org/10.1016/j.aej.2025.02.037>.
- [20] A. Hamza *et al.*, "A chaotic variant of the Golden Jackal Optimizer and its application for medical image segmentation," *Applied Intelligence*, vol. 55, no. 4, Jan. 2025, Art. no. 295, <https://doi.org/10.1007/s10489-024-06084-8>.
- [21] P. K. Sahu and T. Fatma, "Optimized Breast Cancer Classification Using PCA-LASSO Feature Selection and Ensemble Learning Strategies With Optuna Optimization," *IEEE Access*, vol. 13, pp. 35645–35661, 2025, <https://doi.org/10.1109/ACCESS.2025.3539746>.
- [22] K. Clark *et al.*, "The Cancer Imaging Archive (TCIA): Maintaining and Operating a Public Information Repository," *Journal of Digital Imaging*, vol. 26, no. 6, pp. 1045–1057, Dec. 2013, <https://doi.org/10.1007/s10278-013-9622-7>.
- [23] M. Buda, A. Saha, and M. A. Mazurowski, "Association of genomic subtypes of lower-grade gliomas with shape features automatically extracted by a deep learning algorithm," *Computers in Biology and Medicine*, vol. 109, pp. 218–225, Jun. 2019, <https://doi.org/10.1016/j.combiomed.2019.05.002>.
- [24] M. Irfan *et al.*, "Effectiveness of Deep Learning Models for Brain Tumor Classification and Segmentation," *Computers, Materials & Continua*, vol. 76, no. 1, pp. 711–729, 2023, <https://doi.org/10.32604/cmc.2023.038176>.
- [25] A. Kotte and V. K. Prasad, "Hybrid 3D U-Net and Attention Mechanisms for Whole Heart Segmentation from CT Images," *Engineering, Technology & Applied Science Research*, vol. 15, no. 2, pp. 21822–21828, Apr. 2025, <https://doi.org/10.48084/etasr.10115>.
- [26] K. Hamed and U. Ozgunalp, "A Comparative Analysis of Pretrained Models for Brain Tumor Classification and Their Optimization Using Optuna," in *2024 Innovations in Intelligent Systems and Applications Conference (ASYU)*, Ankara, Turkiye, Oct. 2024, pp. 1–7, <https://doi.org/10.1109/ASYU62119.2024.10757117>.
- [27] S. Ghosh, A. Chaki, and K. Santosh, "Improved U-Net architecture with VGG-16 for brain tumor segmentation," *Physical and Engineering Sciences in Medicine*, vol. 44, no. 3, pp. 703–712, Sep. 2021, <https://doi.org/10.1007/s13246-021-01019-w>.
- [28] A. C. Yadav, M. H. Kolekar, Y. Sonawane, G. Kadam, S. Tiwarekar, and D. R. Kalbande, "EffUNet++: A Novel Architecture for Brain Tumor Segmentation Using FLAIR MRI Images," *IEEE Access*, vol. 12, pp. 152430–152443, 2024, <https://doi.org/10.1109/ACCESS.2024.3480271>.

## AUTHOR'S PROFILE

**Thavavel Vaiyapuri** (IEEE Member) is currently an Associate Professor in the Department of Computer Sciences at the College of Computer Engineering and Sciences, Prince Sattam Bin Abdulaziz University. She is a fellow of the HEA, UK. She is also a DELL EMC2-certified associate in cloud computing and big data analytics. She has authored/edited books with renowned publishers such as CRC Press and holds patents to her credit in the field of cybersecurity. With nearly 25 years of research and teaching experience, she has published more than 100 research publications in peer-reviewed journals and international conferences. Her research interests include data science, security, computer vision, and high-performance computing.